

# Understanding local Dwarf Spheroidals and their scaling relations under MOND

X. Hernandez<sup>1,2</sup>, S. Mendoza<sup>1</sup>, T. Suarez<sup>1</sup>, and T. Bernal<sup>1</sup>

<sup>1</sup> Instituto de Astronomía, Universidad Nacional Autónoma de México, AP 70-264, Ciudad Universitaria, Distrito Federal 04510, México

<sup>2</sup> GEPI, Observatoire de Paris, Meudon Cedex, France  
e-mail: xavier,sergio,tsuarez,tbernal@astroscu.unam.mx

12th February 2019

## Abstract

**Aims.** Using a specific form of the interpolation MOND function, we explore some of the consequences for dwarf spheroidal galaxies.

**Methods.** The particular form of the interpolation function used, leads to a law of gravity which naturally accounts for Newtonian and MONDian phenomena. We show that this does not violate dynamical constraints at sub-galactic and solar system scales, does not degrade the good fit of the MOND proposal at large galactic scales, and in fact, slightly improves the accordance with observations at dSph scales. This formalism yields a good description of gravitational phenomena without the need to invoke the presence of the still undetected and hypothetically dominant dark matter.

**Results.** Isothermal equilibrium density profiles then yield projected surface density profiles for the local dSph galaxies in very good agreement with observational determinations, for values of the relevant parameters as inferred from recent observations of these Galactic satellites. The observed scaling relations for these systems are also naturally accounted for within the proposed scheme.

**Conclusions.** The results obtained shed some light into the form that the MOND interpolating function may have for the most challenging regime, which occurs at moderate accelerations and intermediate mass-weighted lengths.

**Key words.** gravitation – galaxies: dwarf — galaxies: kinematics and dynamics – dark matter — Local Group

## 1. Introduction

When Newtonian gravity was first presented, it afforded an elegant and unified description of gravitational phenomena both on earth, and at solar system scales, the universe, for the epoch. The extraordinary success of this description quickly resulted in it being taken as a definitive and final result, a universal law of gravity. The first gravitational anomaly appeared towards the middle of the 19<sup>th</sup> century, with the determination of unexpected

deviations in the orbit of Uranus (Le Verrier 1846). Within the framework of Newtonian gravity, the anomaly was explained as indirect evidence for dark matter, in the sense of “as yet undetected”. Indeed, the planet Neptune was later found, precisely where it was required (Galle 1846). The second appreciable gravitational anomaly was the inexplicable rate at which the perihelion of the planet Mercury precesses (Le Verrier 1846). Again, considering Newtonian gravity to be definitive, an explanation was put forth in the form of more dark matter, this time, the hypothetical planet Vulcan hiding behind the sun (Le Verrier 1859, 1876). The solution was not optimal, and indeed, no such planet exists, this second gravitational anomaly signalled not indirect evidence for undetected matter, but the limit of validity of Newtonian theory (for an excellent review on all this see e.g. Zakharov et al. 2009, and references therein).

Starting from galaxy cluster dynamics as early as the 1930s (Zwicky 1937), and on to rotation curves of spiral galaxies during the later third of the past century (see e.g. Sofue & Rubin 2001, and references therein), a substantial gravitational anomaly has been identified at galactic scales and beyond. The most common explanation, is the dark matter hypothesis. Although it offers a self-consistent explanation of the relevant facts, that no direct detection has been possible, despite decades of experimental searches, and the somewhat uncomfortable fact that it represents not a minor correction to the matter budget (as Neptune did), but a heavily dominant contribution, has resulted in this hypothesis being questioned. It serves to bear in mind that the extrapolation from the solidly established regime of validity of Newtonian gravity (solar system and binary star dynamics) required to reach galactic scales and beyond, is far larger than that required to reach the orbit of Mercury from terrestrial orbit dynamics, by many orders of magnitude.

If one wants to explore a broader parameter space where the existence of dark matter is not a necessity, one must consider variations in the law of gravity at the galactic and extragalactic scales where dark matter has been proposed as dominating the dynamics. The best studied such proposal is the MOND hypothesis of Milgrom (1983), which has been shown to account well for the rotation curves of spiral galaxies (e.g. Sanders & McGaugh 2002), naturally incorporating the Tully-Fisher relation (see e.g. Milgrom 2008, and references therein).

Abundant recent publications of velocity dispersion measurements of stars in the local dSph galaxies, the extended and flat rotation curves of spiral galaxies, the large dispersion velocities of galaxies in clusters, the gravitational lensing due to massive clusters of galaxies, and even the cosmologically inferred matter content for the universe, are successfully modelled under MOND, not as indirect evidence for the existence of a dominant dark matter component, but as direct evidence for the failure of the current Newtonian and General Relativistic theories of gravity, in the large scale or low acceleration regimes relevant for the above. Some recent examples of the above being Milgrom & Sanders (2003), Sanders & Noordermeer (2007), Nipoti et al. (2007), Famaey et al. (2007), Gentile et al. (2007), Tiret et al. (2007), Sánchez-Salcedo et al. (2008).

The range of galactic dynamical problems treated under MOND has extended from the first order gravitational effects of rotation curves and velocity dispersion measurements, to cover a wide range of more subtle problems. Tidal forces, with their role in limiting the sizes

of satellites and, in MOND, establishing escape velocities from satellites or galaxies subject to an external acceleration field were studied by Sanchez-Salcedo & Hernandez (2007). Wu et al. (2008) calculated the escape velocity for the Milky Way under both MOND and dark matter, and concluded that under both hypotheses the LMC appears as bound, in spite of the recently determined high proper motion for this object, with slightly better fits under MOND. Sanchez-Salcedo et al. (2008) looked at the thickness of the extended HI disk of the Milky Way from both angles, and found a somewhat better fit to observations under MOND. Sanchez-Salcedo et. al (2006) and Nipoti et al. (2008) have examined the problem of dynamical friction in dSph galaxies, comparatively under Newtonian gravity and MOND, with decay timescales for globular clusters being somewhat shorter in MOND, a potential problem, unless one admits for large initial orbital radii for the observed globular clusters, beyond the current extent of the stellar populations.

Going to cosmological scales, recently Skordis et al. (2006) studied the cosmic microwave background, Halle et al. (2008) looked at the problem of the cosmic growth of structure, Zhao et al. (2006) studied gravitational lensing of galaxies and Angus et al. (2007) and Milgrom & Sanders (2008) studied dynamics of clusters of galaxies. All of the above finding the MOND description of the problem as a plausible option, within the observational errors of the relevant determinations.

Observationally, it appears that MOND fares as well as dark matter in accounting for measured dynamics, at all but the smallest regimes, the case of local dSph galaxies remains the most controversial. Under Newtonian dynamics some discussion remains regarding the form of the dark halo density profile of these systems, e.g. Peñarrubia et al. (2008) find a cuspy halo to give a good fit to the stellar velocity measurements, while Gilmore et al. (2007) prefer a constant density core, as also found by Hernandez & Gilmore (1998) to yield the long dynamical friction timescales for globular clusters necessary to account for the extended globular cluster systems sometimes observed in local dSphs. However, always under Newtonian dynamics, dSphs are unequivocally inferred to be massively dominated by dark matter halos e.g. Mateo (1998). Published studies in MOND, typically assuming the deep MOND regime, sometimes find that a different value for the acceleration scale of the theory is obtained for different dSph galaxies, when fitting detailed dynamical models to the data (Lokas 2001), or that  $M/L$  ratios remain higher than those of stellar populations, making dark matter necessary even under MOND, e.g. Sanchez-Salcedo & Hernandez (2007). Still, this last point remains somewhat controversial, Angus (2008) suggests the MOND proposal will hold for local dSph galaxies, once the effects of tidal disruption are adequately incorporated.

Regarding corresponding theoretical developments, numerous alternative theories of gravity have recently appeared (Bekenstein 2004, Sanders 2005, Sobouti 2007, Bruneton & Esposito-Farese 2007, Zhao 2007, Arbey 2008), now mostly grounded on geometrical extensions of General Relativity and Field Theory, which lead in the Newtonian limit to laws of gravity which in the large scale or low acceleration regime, reduce to the MOND fitting formulas.

MOND is characterised by a low acceleration regime where dynamics mimic the presence of dark matter, a high acceleration regime where Newtonian gravity is recovered, and a

somewhat ill-defined transition region. In terms of looking for fundamental GR extensions which might reproduce the MOND phenomenology, this last is a cumbersome point which makes matters complicated. In such studies of GR extensions (e.g. Bekenstein 2004, Sobouti 2007, Capozziello et al. 2007, Mendoza & Rosas-Guevara 2007) one often finds that a simple description is sought, but only for the deep MOND regime (e.g. Sobouti 2007, Capozziello et al. 2007), or studies where highly complex multi parametric GR extensions are required, to account for the problem at all scales (e.g. Bekenstein 2004).

We show how the MOND prescription with a suitable interpolation function, as the one used by Bekenstein (2004) and later used by Famaey & Binney (2005), can be written as an addition of both MONDian and Newtonian contributions to the acceleration at all scales. The large differences of scales and magnitudes of the two acceleration terms ensure that the addition does not spoil the good match with observations at any scale. We then test this in the regime which has proven most difficult for MOND, that of local dSph galaxies, where high quality recent observations now available allow for a relative clean test. We find that this interpolation function not only yields acceptable  $M/L$  values for all dSph galaxies, but also provides a natural explanation for all the scalings seen in these Galactic satellites. An interesting correlation between the  $M/L$  ratios inferred and the ages of the stellar populations in local dwarf spheroidal galaxies is found, and naturally accounted for in modified gravity schemes where stars alone account for the gravitational force.

Section (2) gives a brief summary of the interpolation function first explored by Bekenstein (2004), and gives equilibrium isothermal configurations. These are then used in section (3) to model the local dSph galaxies and obtain  $M/L$  ratios, which are found to be consistent with those typical of stellar populations, at the ages of the different dSph systems. Also in section (3) an exploration of the most conspicuous scaling relations for local dSph galaxies is done, finding that Bekenstein's interpolation function naturally accounts for all features found. Our conclusions are summarised in section (5).

## 2. A particular form of the interpolating function in the MOND prescription

In terms of the acceleration  $\mathbf{g}$  felt by a test particle, the MOND proposal is (see e.g. Milgrom 2002):

$$\mu\left(\frac{g}{a_0}\right)\mathbf{g} = \mathbf{g}_N \quad (1)$$

where  $\mathbf{g}_N$  is the acceleration assigned by Newtonian gravity,  $a_0$  an acceleration scale of the theory, and the interpolating function  $\mu(x := g/a_0)$  is an unspecified function which reduces to unity for large values of its argument, and to its argument, for small values of it. In this way, Newtonian gravity is recovered for large values of  $g$ , and in the deep MOND regime one obtains

$$g = (a_0 g_N)^{1/2}. \quad (2)$$

Strictly speaking, we see that MOND is a theory defined only at the limit values for the acceleration. The value of the constant  $a_0$  has been reasonably determined by calibrating the deep MOND regime through observations of rotation velocity curves of large spiral

galaxies (e.g. Sanders & McGaugh 2002). However, the details of the transition region between the two regimes (i.e. the function  $\mu$ ) have proven harder to establish reliably. This is in part natural, as it is not a scalar parameter, but a functional dependence one needs. A number of variants for this function have been proposed (e.g. Famaey & Binney 2005, Zhao 2007, Sanders & Noordermeer 2007), but apparently suitable dynamical systems in the transition region are hard to come by. Astrophysically, to first approximation one tends to find either systems where no dark matter is needed (stellar and planetary systems, globular clusters, vertical dynamics of disk galaxies, galactic bulges and elliptical galaxies), or systems where dark matter is massively dominant (dSph Galactic satellites, rotation curves of spiral galaxies, galaxy groups and clusters, and cosmological observations). Also, the details of the transition region, the function  $\mu(x)$ , are sensitive to the details of the baryonic system one is looking at, such as the assumed mass to light ratios, gas dynamics, or orbital anisotropy of stars, most of which play a marginal role when in the deep MOND regime. As already remarked, this ill-defined transition is cumbersome to handle in attempts to reproduce the MOND phenomenology through simple GR extensions e.g. Sobouti (2007), Capozziello et al. (2007).

Bekenstein (2004) showed that his relativistic extension of TeVeS in the appropriate non-relativistic limits yields the interpolating function

$$\mu(x) = \frac{\sqrt{1 + 4x} - 1}{\sqrt{1 + 4x} + 1}. \quad (3)$$

This particular interpolating function converges to the right limits as  $x \rightarrow 0, \infty$  and has a very peculiar property. Direct substitution of equation (3) into the absolute value of relation (1) yields:

$$g = g_N + (a_0 g_N)^{1/2} \quad (4)$$

This equation can be thought of as a generalised gravity recipe described by the addition of two terms, the first a standard Newtonian acceleration term and the second, the MOND acceleration term. Seen in this way, equation (4) changes it's acceleration behaviour limiting cases to a scale limiting behaviour. Indeed, for the case of a test particle on a gravitational field produced by a central mass  $M$ , located at a distance  $R$  from it, equation (4) can be written as:

$$g = -\frac{GM}{R^2} - \frac{(Ga_0)^{1/2} M^{1/2}}{R}. \quad (5)$$

where  $G$  is Newton's constant of gravity. Seen in this way, equation (5) converges to Newtonian gravity for sufficiently small  $R/M^{1/2}$ 's and reproduces MOND strong limit for sufficiently large  $R/M^{1/2}$ 's, and so the acceleration limits are now "scale-weighted" limits. It is worth noting that equation (5) is certainly the simplest modification to Newtonian gravity once the strong MOND regime is known.

Let us now rewrite equation (4) in such a way that the scale-weighting becomes more clear. To do so, recall that  $g_N = -\nabla\phi_N$ , where  $\phi_N$  represents the standard Newtonian potential and  $g = -\nabla\phi$ , where  $\phi$  is the scalar potential of the gravitational field. With this, equation (4) can be written as:

$$g = g_N (1 + \chi). \quad (6)$$

where  $\chi := (a_0/G)^{1/2} (R/M^{1/2})$ . In what follows we use the standard values of  $a_0 = 1 \times 10^{-8} \text{ cm s}^{-2}$  (Milgrom & Sanders 2008) and  $G = 4.5 \times 10^{-39} M_\odot^{-1} \text{ s}^{-2} \text{ kpc}^3$ , in units suitably chosen for galactic applications.

For terrestrial scales, we take  $M = 3 \times 10^{-6} M_\odot$ ,  $R = 2.07 \times 10^{-13} \text{ kpc}$  to get  $\chi = 3.23 \times 10^{-6}$ . Therefore, the corrections due to the inclusion of the second term in equation (6) to gravitational dynamics on earth are of order  $10^{-6}$ . This does not present any conflict with observations, given that the uncertainty in the determinations of  $G$ , the fundamental physical constant with the largest fractional uncertainty, is of order 1.4 parts in  $10^4$  (e.g, Binney & Tremaine 2008, appendix A).

For solar system scales, we take  $M = 1 M_\odot$ ,  $R = 4.86 \times 10^{-9} \text{ kpc}$  to get  $\chi = 1.3 \times 10^{-4}$  for the orbit of the earth, still within the uncertainties in the value of  $G$  alone. This becomes even smaller in going to the inner solar system, but grows towards the outer solar system, where however, uncertainties in orbital radii and periods also grow substantially, with modern observations extending only for a fraction of the orbital period for the outer planets. Note that some researchers (see e.g. Bekenstein 2006, and references therein) claim that the Pioneer anomaly can be explained by MOND. This assumption can prove wrong if uneven thermal radiation in the spacecrafts is found (Toth & Turyshev 2009) which could possibly be due to the flyby anomaly (Turyshev & Toth 2009). In other words, the MONDIAN approximation appears not to be relevant at solar system scales, where General Relativity and Newtonian Gravity have proven correct (Turyshev 2009; Anderson et al. 2002). On the other hand, as discussed by Milgrom (2009), it is likely that current tests at solar system scales cannot conclusively reach definitive conclusions on the MOND interpolating function.

In going to globular clusters, with  $M = 10^{5-6} M_\odot$ ,  $R = 2 - 10 \times 10^{-3} \text{ kpc}$  we get values for  $\chi$  of between 0.1 and 0.01, this time, the correction becomes smaller than the errors and uncertainties in the observational determinations for the values of radii and masses for globular clusters. For elliptical galaxies and bulges, with masses going from about  $10^9$  to  $10^{11} M_\odot$  and radii of between 0.5 and 10 kpc,  $\chi$  is of order 0.1. We hence see that the correction to gravitational dynamics due to the proposed inclusion of a second term in equation (6) is sufficiently small to have remained undetected, in all systems where no gravitational anomaly is found, and where dynamics are consistent with Newtonian gravity, in the absence of any dark matter.

On the other hand, for systems where the presence of dark matter is inferred, given that this is always inferred to be dominant, the addition of the Newtonian term onto the MOND proposal generally provides a negligible contribution. For example, for the Galactic disk at the solar radius,  $M = 5 \times 10^{10} M_\odot$  and  $R = 8.5 \text{ kpc}$  give  $\chi = 2$ , consistent with an inference of about 50% dark matter within the solar circle. In going to the outskirts of the Milk Way, we go to  $R = 100 \text{ kpc}$ , and hence  $\chi = 20$ , the system is either totally dark matter dominated, or in a regime where the second term in equation (6) almost fully determines the dynamics.

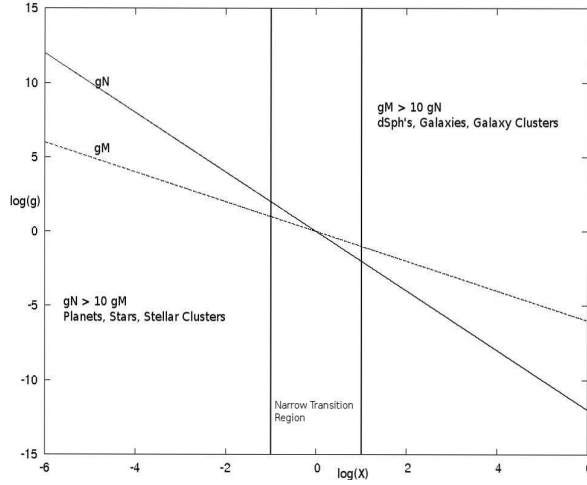


**Figure 1.** Scalings of the Newtonian and MONDian terms in equation (5),  $g_N$  and  $g_M$ , respectively, against the parameter  $\chi$ , normalised to  $g(1)$ . In the region to the left of the first vertical line  $g_N$  dominates over  $g_M$  by upwards of 1 order of magnitude, and is occupied by systems where no dark matter is necessary to explain observed dynamics under Newtonian gravity, which will be modified by less than observational uncertainties by the inclusion of the second term in equation (6). To the right of the second vertical line  $g_M$  dominates over  $g_N$  by upwards of 1 order of magnitude, and is occupied by systems where substantial dark matter is needed to account for the observed dynamics under Newtonian gravity.

An schematic representation is given in Figure (1), which gives a log-log plot of the dependences of Newtonian gravity and deep MOND gravity against the parameter  $\chi$ . We see that the distinct power law dependences ensure that at small values of  $\chi$  the Newtonian term completely dominates, while the opposite holds for large values of  $\chi$ , with a necessarily narrow transition region.

From the form of equation (5), it would be tempting to add the following term of the  $\sim 1/R$  series, a further (perhaps negative) constant term, which would result in an  $\chi^2$  additive term in equation (6). If chosen suitably small, for the same reasons as given above, it would have null effects at all but the largest scales, perhaps as a tool to model the cosmological constant. This extension certainly doesn't correspond to MOND, since no interpolation function  $\mu(X)$  can be constructed. However, in such terms, equation (6) might be interpreted as a series expansion of a more fundamental underlying gravity law, only the first terms of which we have begun to appreciate empirically, as observations probe increasingly higher  $\chi$  regimes, typically corresponding to increasingly larger scales. The introduction of the constant term in equation (5) and its calibration from cosmology however, must be done within a generalised GR framework.

### 2.1. Equilibrium configurations

In order to test stringently the proposed model against observations, we go to the regime which has resulted most troublesome for MOND, the now very well studied dSph galaxies of the local group. To compare against local dSph galaxies, we require the derivation of

equilibrium configurations for a population of self-gravitating stars. We begin by noting that the validity of Newton's theorems for spherically symmetric matter distributions, that the contribution to the force felt by an observer due to external shells vanishes, and that the contribution of all shells interior to the observer is equivalent to concentrating all mass interior to the observer at the centre, holds also under the present proposal. The two theorems depend on the fact that the numerator of the Newtonian term in equation (5) for a fixed solid angle fraction of a thin shell scales with the second power of distance to the shell, as does the denominator. For the second term in equation (5), the numerator scales with  $\sqrt{R^2} = R$ , as does the denominator, assuring the validity of Newton's theorems for spherical mass distributions (e.g. see Bekenstein & Milgrom 1984).

We now write the equation of hydrostatic equilibrium for a polytropic equation of state  $p = K\rho^\gamma$ ,

$$K\gamma\rho^{\gamma-2}\frac{d\rho}{dr} = -\nabla\phi = -\frac{GM(r)}{r^2} - \frac{(a_0/G)^{1/2} M(r)^{1/2}}{r}. \quad (7)$$

Using the fact that  $\rho = (4\pi r^2)^{-1}dM(r)/dr$ , where  $M(r)$  is the mass of the configuration at a radius  $r$ , and going to isothermal conditions,  $K = \sigma^2$  with  $\gamma = 1$ , the previous equation can be written as:

$$\sigma^2 \left[ \left( \frac{dM}{dr} \right)^{-1} \frac{d^2 M}{dr^2} - \frac{2}{r} \right] = -\frac{GM(r)}{r^2} - \frac{(a_0/G)^{1/2} M(r)^{1/2}}{r} \quad (8)$$

In the above second order differential equation for  $M(r)$ , the constant isotropic velocity dispersion for the population of stars has been written as  $\sigma$ . We have taken advantage of the correspondence between hydrostatic equilibrium polytropic configurations, and self gravitating stellar systems, which does not depend on the particular form of the Poisson equation, only on the validity of the isothermal condition for the stellar population, see e.g. Binney & Tremaine (2008).

Taking initial conditions  $M(r) \rightarrow 0$  and  $dM/dr = 4\pi r^2 \rho_0$  for  $r \rightarrow 0$ , a constant central density  $\rho_0$ , we can now solve equation (8) through a numerical finite differences scheme, subject only to two input conditions, a value for  $\sigma$  and a value for  $\rho_0$ .

We can note that neglecting the first term on the right of equation (8), the limit behaviour of  $M(r)$  for large values of  $r$  when the 'MOND' term dominates, is  $\rho \propto r^{-3}$ . Given the presence of the extra Newtonian term, and the long range character of gravity, we can expect full solutions of equation (8) to yield volume density profiles which decay slightly faster than  $r^{-3}$ , and hence, characterised by a finite total mass. In contrast to what happens in Newtonian systems, where isothermal configurations have an infinite total mass, under the proposed gravity law, isothermal self-gravitating configurations will be naturally bound in mass. Hence, there will also be a well defined and finite half mass radius  $R_{\text{hm}}$ , to characterise the resulting equilibrium configurations. Also, as it is the case in MOND, the total mass of the configuration is expected to scale with  $\sigma^4$ . From the dimensional mass scale  $\langle M \rangle \sim \sigma^4 (a_0/G)^{-1}$  one is lead to expect an analog to the Tully-Fisher relation for spheroidal galactic systems, down to the dSph regime.

Figure (2) gives a plot of  $\log(\rho/M_\odot \text{ pc}^{-3})$  vs  $\log(R/\text{kpc})$  for a sample numerical solution to equation (8), for  $\sigma = 7 \text{ km s}^{-1}$  and  $\rho_0 = 0.1 M_\odot \text{ pc}^{-3}$ . We obtain a well defined final



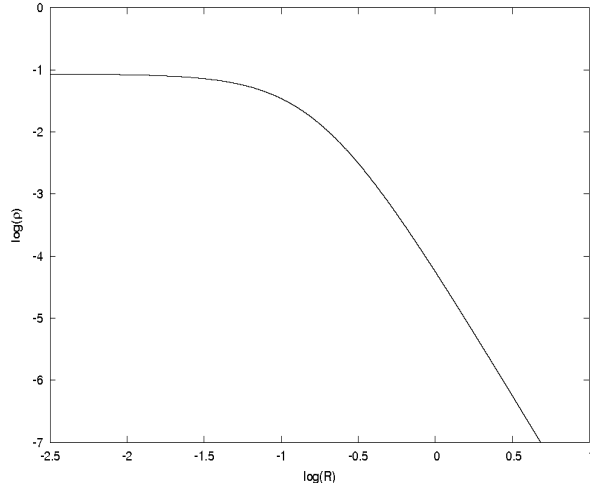


**Figure 2.** A sample isothermal equilibrium density profile, for  $\rho_0 = 0.1 M_\odot pc^{-3}$  and  $\sigma = 7 km/s$ , resulting in a total mass of  $3 \times 10^6 M_\odot$  and a volume half-mass radius of 0.39 kpc. The density is measured in units of  $M_\odot pc^{-3}$  and the distance in units of kpc.

resulting total mass,  $M_{tot}$ , of  $3 \times 10^6 M_\odot$ , and a final volume half-mass radius of 0.39 kpc. We see the expected decay of the density profile at large radii, slightly faster than  $r^{-3}$ . It is this type of density profiles which will be used in the following section to model the local dSph galaxies.

### 3. Local Dwarf Spheroidal Galaxies

As discussed above, once values for the velocity dispersion and the central density are given, numerically solving equation (8) yields the full equilibrium density profile. To now model dSph galaxies, we take values for the reported velocity dispersions for these systems, which hence fix one of the two parameters of the model. A resulting density profile is then integrated along one dimension, to yield a surface density profile, from which the projected half-mass radius is measured. This provides a second constraint, we then vary the value of the input central density to ensure that the resulting half-mass radius  $R_{hm}$  matches the reported half-light radius  $R_{hl}$  of a given dSph. Observational determinations of the velocity dispersion and the half-light radius of a certain dSph galaxy then fully determine the model. Dividing the total mass for the resulting model  $M_{tot}$  by the reported total luminosity  $L_{tot}$  of a dSph, yields a mass to light ratio for the model. Values of the half-light radii and total luminosities were taken from Gilmore et al. (2007), who summarise published results from the references given in Table (1), except for Ursa Minor, where we took the revised value for  $L_{tot}$  from Palma et al. (2003).

Although other stellar systems show velocity dispersion profiles which generally decay as the radial coordinate increases, e.g. globular clusters, the case for observed dSph galaxies is different, with these systems showing essentially flat velocity dispersion profiles, e.g. Gilmore et al. (2007). In cases where some drop in the velocity dispersion profile is observed, this typically occurs towards the edge of the galaxy, affecting only a very small percentage of the total mass of the system. The constancy of these observed velocity dispersion profiles

validates the use of equation (8) under isothermal conditions for the modelling of local dSph's, under the proposed model. We have not at this point attempted a more detailed modelling considering non-isothermal conditions, for example including orbital anisotropy. Although such models are now common in models of dSph galaxies under Newtonian (e.g. Lokas (2002)) or MOND frameworks (e.g. Angus (2008)), and could be included in subsequent analysis. We point to the work by Gilmore et al. (2007), in which isothermal conditions are used to model local dSph galaxies under Newtonian gravity.

Values of  $\sigma$  were taken from adjusting a constant level to the  $\sigma$  profiles of Angus (2008), which are to a very good approximation flat, with the exception of Ursa Minor which shows a significant decrease with increasing radial distances. This galaxy also shows internal structure in phase space at small radii, which might partly account for the steep increase in  $\sigma$  seen by Angus (2008) towards the centre. We have taken a value for  $\sigma$  representative of the situation at around the half-light radius. If however, a strong radial dependence of  $\sigma$  in Ursa Minor were confirmed, this system would have to be excluded from the present sample, as it would then be in conflict with the simple isothermal modelling we are performing here.

Table (1) gives our results for the 8 best studied local dSph galaxies. The values of  $M/L$  we obtain are mostly comparable to those obtained by Angus (2008) for the same systems, but a slight systematic decrease is evident, consistent with having included a further force term, the Newtonian component, which reduced inferred  $M/L$  ratios even further. In general, the values of the parameter  $\langle \chi \rangle$  found, calculated from the resulting model total mass as  $(a_0/G)^{1/2}(2^{1/2}R_{\text{hl}}/M_{\text{tot}}^{1/2})$ , explain why the addition of the Newtonian term is required to fully account for the dynamics. Further, the large range of values of  $\langle \chi \rangle$  shown in the table, explains why sometimes a different  $a_0$  has been found for various dSph's, when fitting dynamics under pure MOND, e.g. Lokas (2001).

The case where the effect of the second term in equation (6) is largest is that of Draco, where the compact configuration and relatively high  $\sigma$  values allow the Newtonian term to figure somewhat more, leading to an important decrease of the inferred  $M/L$  of between 8.1 and 30.9, with respect to the Angus (2008) results of  $M/L$  between 22.6 and 72.9. With the possible exception of Fornax and Sculptor, cases where the reported King core radius serves only as a lower limit for the projected  $R_{\text{hl}}$ , the value for the parameter  $\langle \chi \rangle$  for Draco is the lowest in the sample. This naturally explains why it is here where our results for  $M/L$  differ most, and show a significant reduction with respect to the results of Angus (2008) who takes a  $\mu$  function which rapidly converges to the deep MOND regime, as it is this parameter which determines the relative importance of the Newtonian and MONDian terms in equation (6).

The  $1\sigma$  confidence intervals of our results are only lower bounds, as their calculation includes only uncertainties in the adopted values of  $\sigma$ , and not observational errors in total luminosities and half-mass radii. Also, freedom in the light profile functional fitting would increase our confidence intervals slightly, e.g. the reported  $R_{\text{hl}}$  values for Ursa Minor, Fornax and Sculptor are only lower bounds, as for those galaxies the quantity available is the core radius from King profile fits. Still, this last is only a second order effect, as our

**Table 1.** Basic properties and resulting  $M/L$  ratios for the sample of dSph galaxies.

Galaxy	$\sigma$ [km/s]	$R_{\text{hl}}$ [kpc]	$L_{\text{tot}} \times 10^5 L_{\odot}$	$(M/L)_A$	$(M/L)$	$\langle \chi \rangle$	Age of Youngest Component [Gyr]
Carina	$7 \pm 1.8$	0.290	4.3	$5.6^{+5.2}_{-2.9}$	$6.8^{+8.3}_{-4.6}$	7	3
Draco	$8 \pm 1.5$	0.230	2.6	$43.9^{+29}_{-19.3}$	$17.0^{+13.9}_{-8.9}$	4.1	10
LeoI	$8 \pm 1.2$	0.330	48.0	$0.7^{+0.65}_{-0.3}$	$1.0^{+0.6}_{-0.44}$	5.7	2
Sextans	$7 \pm 1.0$	0.630	5.0	$9.2^{+5.3}_{-3.0}$	$6.3^{+4.2}_{-2.8}$	13.4	(2-6)
Fornax	$12 \pm 1.3$	0.400	150.0	$1.4^{+0.45}_{-0.35}$	$1.4^{+0.6}_{-0.4}$	$> 3.4$	(2-3)
Sculptor	$9.5 \pm 1.7$	0.160	22.0	$3.7^{+2.2}_{-1.4}$	$3.4^{+2.1}_{-0.7}$	$> 2.2$	$> 5$
LeoII	$6 \pm 1.4$	0.185	7.0	$1.85^{+2}_{-1.1}$	$2.3^{+2.4}_{-0.4}$	5.5	6.5
Ursa Minor	$8 \pm 2$	0.300	5.8	$5.8^{+6.5}_{-3.6}$	$8.0^{+9.8}_{-5.1}$	$> 5.3$	12

$(M/L)_A$  gives the values for the mass to light ratios calculated by Angus (2008) under standard MOND and  $M/L$  those in this study under the proposed model. Total luminosities (in the  $V$  band) and half-light radii are from Wilkinson et al. (2006), Wilkinson et al. (2004), Koch et al. (2007), Kleya et al. (2004), Walker et al. (2006), Mateo (1998), Coleman et al. (2007) and Irwin & Hatzidimitriou (1995), for the galaxies in the Table, in the order given, as summarised in Gilmore et al. (2007). Velocity dispersions are from adjusting a constant value to the data of Angus (2008).  $\langle \chi \rangle$  gives the average value of the parameter  $\chi$  as defined in section (2), which measures the relative relevance of the Newtonian and MONDian terms in equation (6). The final column gives an estimate of the age of the youngest stellar population present in each of the systems, allowing an interpretation of the inferred  $M/L$  values in terms of stellar evolution, for Carina, Ursa Minor, LeoI and LeoII from Hernandez et al. (2000), for Fornax from Coleman & de Jong (2008), for Draco from Aparicio et al. (2001), for Sextans from Lee et al. (2003) and for Sculptor from Babusiaux et al. (2005).

inferred  $M/L$  values are not very sensitive to the values of  $R_{\text{hl}}$  used, provided this does not change by a large factor (see the following section).

As expected, the main determinant of the resulting total mass of a numerical solution of equation (8), is the input  $\sigma$ . We find, as expected from the situation of the ‘deep MOND regime’, a strong correlation, with the resulting scaling for all galaxies being well described by:

$$M_{\text{tot}} = \frac{(5.5\sigma^2)^2}{a_0 G}. \quad (9)$$

This could be seen as an extension of the Tully-Fisher relation down to the smallest galactic scales, a natural consequence of the model being explored.

Considering the large  $M/L$  values natural for old stellar populations, e.g. Queloz et al. (1995), Romanowsky et al. (2003), who find  $M/L$  ratios for old stellar populations as high as 7 or 8, our new results are now at the limit of compatibility with  $M/L$  ratios for old naked stellar populations, for all the well studied local dSph galaxies. This holds comfortably for all galaxies except Draco, where compatibility is found only just at the  $1\sigma$  level for our lower limits on the confidence intervals. Hence, our model yields equilibrium isothermal configurations able to explain the observed dynamics of the local dSph galaxies, without the need of dark matter.

A consistency check of the above interpretation is available from the comparison of the  $M/L$  ratios we found, and the age of the youngest stellar population found in each of the galaxies, as inferred from the direct studies of the observed CMDs of the galaxies in question, given in the last column of Table (1). It is reassuring that the highest values for our inferred  $M/L$  ratios, for Ursa Minor and Draco coincide with the galaxies showing no star formation over the last 10 Gyr, the oldest galaxies in the sample, while the lowest values for  $M/L$  are obtained for Leo I and Fornax, the youngest galaxies in the sample with stellar populations as young as 2 Gyr. For the remainder of the sample, galaxies showing their youngest stars at intermediate ages, we find the intermediate values for  $M/L$ . The interpretation of the dynamics under the proposed model is hence in accordance with the natural increase in the  $M/L$  ratios of stellar populations due to the ageing of stars and the consequent build up of black holes, neutron stars and white dwarfs.

As a second consistency check, we now show the resulting projected surface density mass profile for a model of the Leo II galaxy, normalised by the total luminosity of that system. We construct the surface brightness profile using our model for an equilibrium isothermal system having velocity dispersion and projected  $R_{\text{hm}}$  (assumed equal to the observed  $R_{\text{hl}}$ ), equal to those observed for Leo II. This is given in Figure (3), where we have also plotted the observation for the actual surface density light profile of Leo II, from the star counts analysis of Coleman et al. (2007), out to the radius where measurements fall below the background noise level, both normalised to the same total luminosity. We note that the error bars of Coleman et al. (2007) are only a lower estimate of the confidence intervals for this comparison, as they refer only to the errors in the measured star counts, and not to full surface density profile inferences. A very good agreement is evident, showing the proposed models are a good, fully self-consistent representation of the dynamics and both the integral and spatially resolved light distribution in the well studied local dSph galaxies.

#### 4. Scaling relations

We now turn to the scalings shown by the dSph galaxies in our sample. Firstly, we show in Figure (4) the behaviour of the equilibrium isothermal configurations we are solving for, in terms of the resulting projected  $R_{\text{hm}}$  as a function of the input value of  $\rho_0$ , at a constant value of  $\sigma = 10\text{km/s}$ . The remarkable feature of Figure (4) is that after decreasing as  $\rho_0$  increases, when  $\rho_0$  reaches a value of about  $0.3M_{\odot}\text{pc}^{-3}$ , the resulting  $R_{\text{hm}}$  stops changing and settles to a relatively constant value of around 150pc, below which, it does not fall

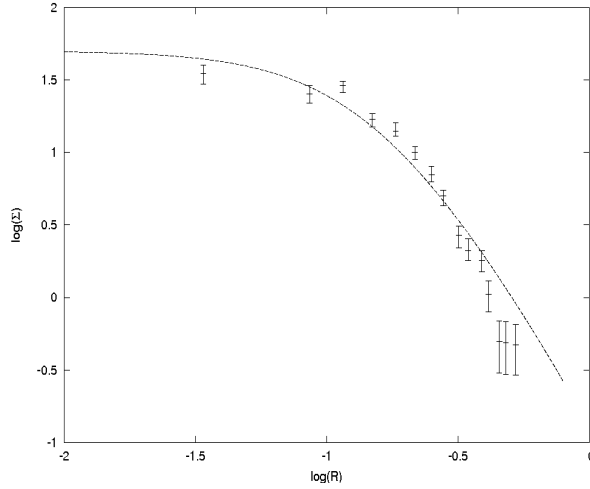


**Figure 3.** Comparison of our projected surface density profile for an equilibrium isothermal solution to equation (8), having input  $\sigma$  and projected  $R_{\text{hm}}$  as the observationally determined values for LeoII, dashed curve. For comparison, we give also the star counts surface density profile for Leo II of Coleman et al. (2007). Both profiles have been normalised to the same total luminosity.

further. This is qualitatively reproduced at all values of  $\sigma$ , with only small changes in the minimum values of  $R_{\text{hm}}$ , for  $\sigma$  in the range of values observed for local dSph galaxies. This is interesting, as it offers a natural explanation for the fact that local dSph galaxies indeed show a minimum lower value for their projected half-light radii, of around 150pc, with most lying around a factor of 2 above this critical limit, as noticed by Gilmore et al. (2007) and seen from Table (1). Indeed, all our models constrained by the observational values of  $\sigma$  and  $R_{\text{hl}}$  for the local dSph's, occur within the flat region of the  $R_{\text{hm}}$  vs.  $\rho_0$  space.

We can now try to understand the assigned Newtonian values of  $M/L$  for local dSph galaxies, and the scalings they show with total luminosity, or absolute magnitude, e.g. Mateo (1998), Gilmore et al. (2007). The assigned Newtonian values of  $M/L$  will never be far from (e.g. Gilmore et al. (2007)):

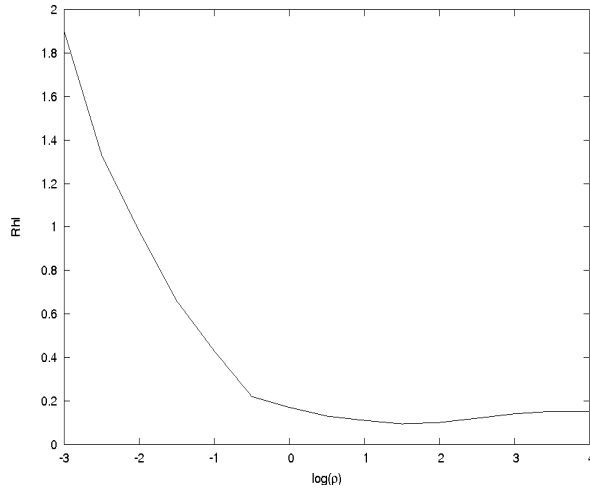
$$(M/L)_N = \left( \frac{10\sigma^2 R_{\text{hl}}}{G} \right) \left( \frac{1}{L_{\text{tot}}} \right). \quad (10)$$

Given our results of the previous section, or alternatively taking as an empirical fact the observed  $R_{\text{hl}}$  of around 300pc, we can evaluate the above equation to first order at  $R_{\text{hl}} = 0.3$ . Also, for an average old stellar population we can take a constant  $M/L$  value of 5 as a representative value for the local dSph's, as our inferences yield, and replace  $\sigma^2$  in equation (9) for the corresponding value through equation (10) to yield:

$$(M/L)_N = \left( \frac{3\sqrt{5}}{5.5} \right) \left( \frac{a_0}{G} \right)^{1/2} \left( \frac{1}{L_{\text{tot}}} \right)^{1/2}. \quad (11)$$

Introducing the absolute magnitude  $M_V = -2.5\log(L_{\text{tot}}) + 4.83$ , and taking the logarithm of the above equation gives:

$$\log(M/L)_N = 3.77 + 0.2M_V. \quad (12)$$



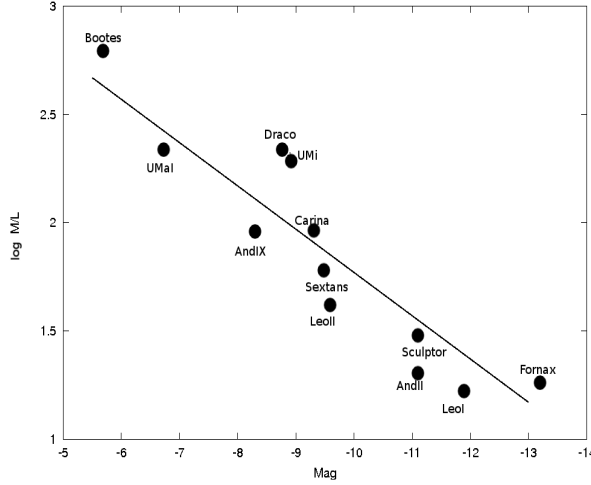
**Figure 4.** Dependence of the resulting projected half-mass radius in kpc, against the assumed central density in  $M_{\odot}\text{pc}^{-3}$ , for isothermal equilibrium configurations under the proposed MOND approximation, at fixed  $\sigma = 10\text{km/s}$ . A very broad region where  $R_{\text{hm}}$  remains almost constant is evident, at precisely the level found to define the minimum  $R_{\text{hl}}$  values for observed dSph galaxies, which have typical values of  $\sigma \simeq 10\text{km/s}$ .

Figure (5) now gives a plot of equation (12), superimposed on recent determinations of the Newtonian  $M/L$  values for a larger sample of local dSph galaxies. Estimates and data as summarised in Gilmore et al. (2007) and references therein, Côté et al. (1999) for And II and Chapman et al. (2005) for And IX, with the value for Sculptor revised upwards to close to 30 from Angus (2008). The good match is evident, extending for over 8 orders of magnitude in  $M_V$ , even more remarkable as the trend found extends for several orders of magnitude further towards the smallest newly discovered dSph systems (G. Gilmore, private communication).

We see that the expectations of the model for the inferred Newtonian  $M/L$  values of local dSph galaxies, modelled as equilibrium isothermal solutions to equation (8), and having typical radii of close to  $0.3\text{kpc}$ , agree very well with independent measurements. The remaining scatter in Figure (5) is compatible with the variations in the actual intrinsic  $M/L$  values for the individual galaxies, and variations of  $R_{\text{hl}}$  around the average  $0.3\text{kpc}$  used in equation (12), which is not a fit to the data, but a first order estimate within our prescription. A very simple explanation for the  $(M/L)_N$  values assigned to all well studied dSph's is hence naturally afforded by our assumptions for the most average intrinsic  $M/L$  and  $R_{\text{hl}}$  values, without the need to invoke complex astrophysical processes (e.g. tidal disruption, strong outflows, etc.) or to fine tune any parameters.

## 5. Conclusions

We have used a MOND interpolation function which can be seen as the addition of both Newtonian and MONDian acceleration components at all scales (Bekenstein (2004)). For the local dSph galaxies, where MOND results have been most controversial, we show that agreement is improved, and no dark matter is now needed, thanks to the use of a particular



**Figure 5.** Logarithms of the Newtonian  $M/L$  values of local dSph galaxies, from Gilmore et al. (2007), against total observed  $V$  band magnitudes. The straight line gives the Newtonian  $M/L$  values which would be assigned to isothermal equilibrium populations of stars having a constant intrinsic stellar  $M/L$  ratio of 5, and a constant half-mass radius of 300kpc, consistent with what is observed, and to what the proposed model yields for equilibrium configurations having velocity dispersions of 10km/s, as the observed dSph show, according to the model presented here.

$\mu(x)$ . The resulting  $M/L$  ratios are in qualitative accordance with the relative youth of the stellar populations of the individual dSph galaxies, for the sample studied. The observed scalings in  $R_{\text{hl}}$  and assigned  $(M/L)_N$  values as a function of total magnitudes are explained naturally.

*Acknowledgements.* We would like to thank Benoit Famaey, Moti Milgrom and Jacob Bekenstein for fruitful comments made in connection to a previous version of this article. This work was supported in part through two DGAPA-UNAM grants (PAPIIT IN-113007-3 and IN-114107). SM and TB gratefully acknowledge support from DGAPA (IN119203-3) at Universidad Nacional Autónoma de México (UNAM). SM acknowledges financial support granted by CONACyT (26344). TB thanks support from CONACyT (207529).

## References

- Anderson, J. D., Lau, E. L., Turyshv, S., Williams, J. G., & Nieto, M. M. 2002, in Bulletin of the American Astronomical Society, Vol. 34, Bulletin of the American Astronomical Society, 660–+
- Angus, G. W. 2008, MNRAS, 387, 1481
- Aparicio, A., Carrera, R., & Martínez-Delgado, D. 2001, AJ, 122, 2524
- Babusiaux, C., Gilmore, G., & Irwin, M. 2005, MNRAS, 359, 985
- Bekenstein, J. 2006, Contemporary Physics, 47, 387
- Bekenstein, J. D. 2004, Phys. Rev. D, 70, 083509
- Chapman, S. C., Ibata, R., Lewis, G. F., et al. 2005, ApJ, 632, L87
- Coleman, M. G. & de Jong, J. T. A. 2008, ApJ, 685, 933
- Coleman, M. G., Jordi, K., Rix, H.-W., Grebel, E. K., & Koch, A. 2007, AJ, 134, 1938
- Côté, P., Mateo, M., Olszewski, E. W., & Cook, K. H. 1999, ApJ, 526, 147
- Famaey, B. & Binney, J. 2005, MNRAS, 363, 603
- Famaey, B., Gentile, G., Bruneton, J.-P., & Zhao, H. 2007, Phys. Rev. D, 75, 063002

- Galle, J. G. 1846, MNRAS, 7, 153
- Gentile, G., Famaey, B., Combes, F., et al. 2007, A&A, 472, L25
- Gilmore, G., Wilkinson, M. I., Wyse, R. F. G., et al. 2007, ApJ, 663, 948
- Hernandez, X., Gilmore, G., & Valls-Gabaud, D. 2000, MNRAS, 317, 831
- Irwin, M. & Hatzidimitriou, D. 1995, MNRAS, 277, 1354
- Kleyna, J. T., Wilkinson, M. I., Evans, N. W., & Gilmore, G. 2004, MNRAS, 354, L66
- Koch, A., Wilkinson, M. I., Kleyna, J. T., et al. 2007, ApJ, 657, 241
- Le Verrier. 1846, Comptes Rendu, 31
- Le Verrier, U. 1859, R. Acad. Sci. Paris, 59, 379
- Le Verrier, U. 1876, R. Acad. Sci. Paris, 83, 576
- Lee, M. G., Park, H. S., Park, J.-H., et al. 2003, AJ, 126, 2840
- Lokas, E. L. 2001, MNRAS, 327, L21
- Lokas, E. L. 2002, MNRAS, 333, 697
- Mateo, M. L. 1998, ARA&A, 36, 435
- Milgrom, M. 1983, ApJ, 270, 365
- Milgrom, M. 2008, ArXiv e-prints
- Milgrom, M. 2009, MNRAS, 1143
- Milgrom, M. & Sanders, R. H. 2003, ApJ, 599, L25
- Milgrom, M. & Sanders, R. H. 2008, ApJ, 678, 131
- Nipoti, C., Londrillo, P., Zhao, H., & Ciotti, L. 2007, MNRAS, 379, 597
- Palma, C., Majewski, S. R., Siegel, M. H., et al. 2003, AJ, 125, 1352
- Queloz, D., Dubath, P., & Pasquini, L. 1995, A&A, 300, 31
- Romanowsky, A. J., Douglas, N. G., Arnaboldi, M., et al. 2003, Science, 301, 1696
- Sánchez-Salcedo, F. J., Saha, K., & Narayan, C. A. 2008, MNRAS, 385, 1585
- Sanders, R. H. & McGaugh, S. S. 2002, ARA&A, 40, 263
- Sanders, R. H. & Noordermeer, E. 2007, MNRAS, 379, 702
- Sofue, Y. & Rubin, V. 2001, ARA&A, 39, 137
- Tiret, O., Combes, F., Angus, G. W., Famaey, B., & Zhao, H. S. 2007, A&A, 476, L1
- Toth, V. T. & Turyshchev, S. G. 2009, Phys. Rev. D, 79, 043011
- Turyshchev, S. G. 2009, Physics Uspekhi, 52, 1
- Turyshchev, S. G. & Toth, V. T. 2009, Space Science Reviews, 86
- Walker, M. G., Mateo, M., Olszewski, E. W., et al. 2006, AJ, 131, 2114
- Wilkinson, M. I., Kleyna, J. T., Evans, N. W., et al. 2004, ApJ, 611, L21
- Wilkinson, M. I., Kleyna, J. T., Wyn Evans, N., et al. 2006, in EAS Publications Series, Vol. 20, EAS Publications Series, ed. G. A. Mamon, F. Combes, C. Deffayet, & B. Fort, 105–112
- Zakharov, A. F., Capozziello, S., de Paolis, F., Ingrosso, G., & Nucita, A. A. 2009, Space Science Reviews, 19
- Zwicky, F. 1937, ApJ, 86, 217